

DISCLAIMER

This report was prepared as an account of work sponsored by an agency of the United States Government. Neither the United States Government nor any agency thereof, nor any of their employees, makes any warranty, express or implied, or assumes any legal liability or responsibility for the accuracy, completeness, or usefulness of any information, apparatus, product, or process disclosed, or represents that its use would not infringe privately owned rights. Reference herein to any specific commercial product, process, or service by trade name, trademark, manufacturer, or otherwise does not necessarily constitute or imply its endorsement, recommendation, or favoring by the United States Government or any agency thereof. The views and opinions of authors expressed herein do not necessarily state or reflect those of the United States Government or any agency thereof. Reference herein to any social initiative (including but not limited to Diversity, Equity, and Inclusion (DEI); Community Benefits Plans (CBP); Justice 40; etc.) is made by the Author independent of any current requirement by the United States Government and does not constitute or imply endorsement, recommendation, or support by the United States Government or any agency thereof.

SANDIA REPORT

SAND2025-12361

Printed September 2025

Sandia
National
Laboratories

ThunderDOEME: A Seismoacoustic Deployment at Langmuir Observatory

Clinton D. Koch, Michael Fleigle, Nora Wynn

Prepared by
Sandia National Laboratories
Albuquerque, New Mexico
87185 and Livermore,
California 94550

Issued by Sandia National Laboratories, operated for the United States Department of Energy by National Technology & Engineering Solutions of Sandia, LLC.

NOTICE: This report was prepared as an account of work sponsored by an agency of the United States Government. Neither the United States Government, nor any agency thereof, nor any of their employees, nor any of their contractors, subcontractors, or their employees, make any warranty, express or implied, or assume any legal liability or responsibility for the accuracy, completeness, or usefulness of any information, apparatus, product, or process disclosed, or represent that its use would not infringe privately owned rights. Reference herein to any specific commercial product, process, or service by trade name, trademark, manufacturer, or otherwise, does not necessarily constitute or imply its endorsement, recommendation, or favoring by the United States Government, any agency thereof, or any of their contractors or subcontractors. The views and opinions expressed herein do not necessarily state or reflect those of the United States Government, any agency thereof, or any of their contractors.

Printed in the United States of America. This report has been reproduced directly from the best available copy.

Available to DOE and DOE contractors from

U.S. Department of Energy
Office of Scientific and Technical Information
P.O. Box 62
Oak Ridge, TN 37831

Telephone: (865) 576-8401
Facsimile: (865) 576-5728
E-Mail: reports@osti.gov
Online ordering: <http://www.osti.gov/scitech>

Available to the public from

U.S. Department of Commerce
National Technical Information Service
5301 Shawnee Rd
Alexandria, VA 22312

Telephone: (800) 553-6847
Facsimile: (703) 605-6900
E-Mail: orders@ntis.gov
Online order: <https://classic.ntis.gov/help/order-methods/>



ABSTRACT

This report documents a two-month deployment of seismoacoustic instrumentation at the Langmuir Observatory, located outside Socorro, New Mexico. A total of eleven Fairfield Nodal Seismometers and fifteen GEM infrasound loggers were deployed from June 2 to August 5, 2025. The nodal seismometers recorded data for an average of 34 days, while the GEMs had variable operational durations throughout the deployment period. The primary objective was to capture thunder signals using seismoacoustic instrumentation, contributing to a better understanding of the acoustic and seismic phenomena associated with thunder.

Coinciding with this deployment, optical and electric field sensors were present, providing information regarding the timing and location of lightning strikes in the region. Additionally, triggered lightning strikes were conducted, serving as a ground truth for validating the captured thunder signals. Preliminary analysis of the data reveals clear thunder signals in both the seismic and infrasound recordings, with peak frequencies observed across a range of 4 to 40 Hz, depending on the event.

ACKNOWLEDGEMENTS

The authors greatly appreciate and acknowledge Andy Scholand and Adonis Leal for their assistance in understanding the electric field and optical data as well as in the organization and execution of the deployment. We also greatly appreciate and acknowledge Andrea Conley for her time and effort in providing a technical review of this work. SandiaAI was used in the preparation of this report.

Sandia National Laboratories is a multimission laboratory managed and operated by National Technology & Engineering Solutions of Sandia, LLC, a wholly owned subsidiary of Honeywell International Inc., for the U.S. Department of Energy's National Nuclear Security Administration under contract DE-NA0003525.

CONTENTS

Abstract.....	3
Acknowledgements.....	4
Acronyms and Terms	7
1. Introduction	9
2. Deployment.....	10
3. Data	13
4. Conclusions.....	16
References	17
Distribution.....	19

LIST OF FIGURES

Figure 1: Map view of ThunderDOEME deployment. Station labels in white are those that recorded while those in red failed to record.....	11
Figure 2: Data continuity for seismic (left) and infrasound (right) stations. Vertical redlines indicate gaps in the data; blue lines indicate continuous data. Green x's indicate a new day.	11
Figure 3: Record section showing infrasound and seismic waveforms following the June 10th 21:04 UTC triggered lightning strike. Distances are calculated using the surface location of the rocket launch as the origin location and an origin time (red line) estimate based of electromagnetic instrumentation. Traces filtered using a 1–25 Hz bandpass. Distances are sorted sequentially by increasing distance, but relative distance is not incorporated to clearly show the individual waveforms.	13
Figure 4: Record section showing infrasound and seismic waveforms following the June 10 th 21:06 UTC triggered lightning strike. All other parameters are as in Figure 3.....	14
Figure 5: Record section showing infrasound waveforms following the July 18th 19:45 UTC triggered lightning strike. All other parameters are as in Figure 3.....	14
Figure 6: Infrasound and seismic waveforms for a 30-minute period during a thunderstorm on June 11th. Dashed red lines indicate lightning detections from electric field instrumentation....	15

LIST OF TABLES

Table 1: Deployment details for the ThunderDOEME deployment.....	11
--	----

This page left blank

ACRONYMS AND TERMS

Acronym/Term	Definition
GEM	GEM infrasound Logger
Node	Fairfield ZLand Nodal Seismometer

This page left blank

1. INTRODUCTION

This report describes a deployment of seismic and acoustic sensors near the Langmuir Observatory in the Magdalena Mountains southwest of Socorro, New Mexico. The primary focus of the deployment is to obtain data that can enhance the characterization of the seismoacoustic properties of thunder signals. The study of thunder signals is important for various scientific and practical applications, including the discrimination between natural and man-made sources, site characterization, and a better understanding of potential noise sources.

Thunder is produced by the rapid expansion of air due to extreme heating from lightning discharges. Farges et al. (2021) demonstrated that infrasound measurements from thunderstorms can be effectively correlated with lightning activity, highlighting the utility of infrasound in understanding atmospheric dynamics and thunderstorm characteristics. Similarly, a large-N deployment was used to detect thunderstorms at distances up to 900 km (Scamfer and Anderson, 2023). Recent literature highlights a growing interest in the acoustic and seismic phenomena associated with thunder events. Studies by Lin and Langston (2007; 2009a, 2009b) utilized an array of infrasound and seismic sensors to analyze thunder signals, demonstrating their potential for characterizing shallow velocity site responses. Hong et al. (2023) focused on seismic waves induced by thunder in urban environments, providing a theoretical framework for inverting thunder source spectra and revealing that these seismic signals can mimic ground motions comparable to moderate earthquakes.

Collectively, these studies underscore the potential of both infrasound and seismic monitoring to enhance our understanding of thunder phenomena, offering insights into the acoustic-to-seismic coupling mechanisms and their implications for hazard assessments. However, thunder can also be a nuisance source, often difficult to distinguish from other natural or man-made sources. Therefore, better characterization of thunder sources recorded on multiple arrays is crucial for effective source discrimination.

Seismic and infrasound stations were deployed near the Langmuir Observatory, located at an elevation of 3,240 meters in the Magdalena Mountains, approximately 27 kilometers southwest of Socorro. This deployment coincides with the installation of optical and electric field instruments at and around Langmuir, which provide valuable ground truth for the timing, location, and type of lightning strikes causing the thunder. While this report focuses solely on the seismoacoustic deployment, the concurrent deployment of other instruments presents an opportunity for multi-phenomenological studies, further enriching our understanding of thunder signals and their implications.

2. DEPLOYMENT

From June 3rd to August 5th, a deployment of GEM infrasound loggers (GEM) and Fairfield ZLand nodal seismometers (nodes) was conducted to monitor thunder sources around Langmuir Observatory. This deployment involved a total of 15 infrasound GEMs (Anderson et al., 2018) and 11 Fairfield ZLand nodal seismometers, organized into three small-aperture seismoacoustic arrays and one larger-aperture array (Figure 1). The three small-aperture arrays were configured with three elements arranged in a triangular formation, with an approximate spacing of 100 meters between each element. The intent with this arrangement is to create a flexible deployment where different array sizes are sensitive to different frequencies. The central and southern small-aperture arrays were equipped with three GEM loggers and a single seismic node. Notably, in the southern small-aperture array, only one GEM and seismic node recorded successfully, while the other GEMs failed to capture data. In contrast, the northern small-aperture array featured four GEMs, each co-located with a seismic node; however, one of the nodes in this array also failed to record. The larger-aperture array was designed to cover a more extensive area, measuring approximately 1.9 by 3.7 kilometers. Each element of this array included both a seismic node and an infrasound GEM, allowing for comprehensive data collection across a broader spatial range (Figure 1).

The GEMs recorded at 100 Hz and utilized solar power for operation. This arrangement resulted in variable coverage throughout the deployment period. The GEMs instrument response has corner frequencies corresponding to -3 dB attenuation at 0.039 and 27.1 Hz. While some sensors recorded continuously for the entire duration, others experienced interruptions (Figure 2). Four GEMs, SIG31, SIG32, ESLRI, and EOBSI, failed to record data altogether. The loss of these instruments impacts the design of the arrays. The southernmost small array is reduced to a single infrasound instrument, and the larger-aperture array is reduced in size. However, the remaining instruments can be incorporated into the larger-aperture array as needed to minimize the loss.

The seismometers, which are 5-Hz, three-component sensors, recorded at 1000 Hz for an average of 33 days, maintaining continuous operation while active. However, one seismometer, SSN11, was unable to deploy successfully. All seismometers were buried except for SSN21, which was partially buried and covered with rocks. The deployment's operational continuity is illustrated in Figure 2.

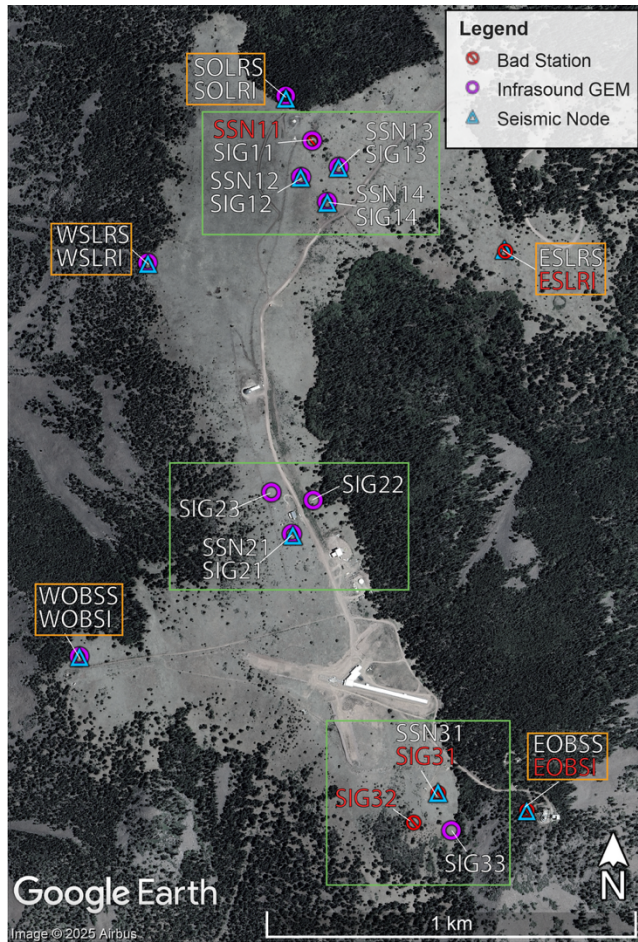


Figure 1: Map view of ThunderDOEME deployment. Instrument labels in white are those that recorded, while those in red failed to record. Green boxes indicate the small arrays, and orange boxes indicate elements of the larger array.

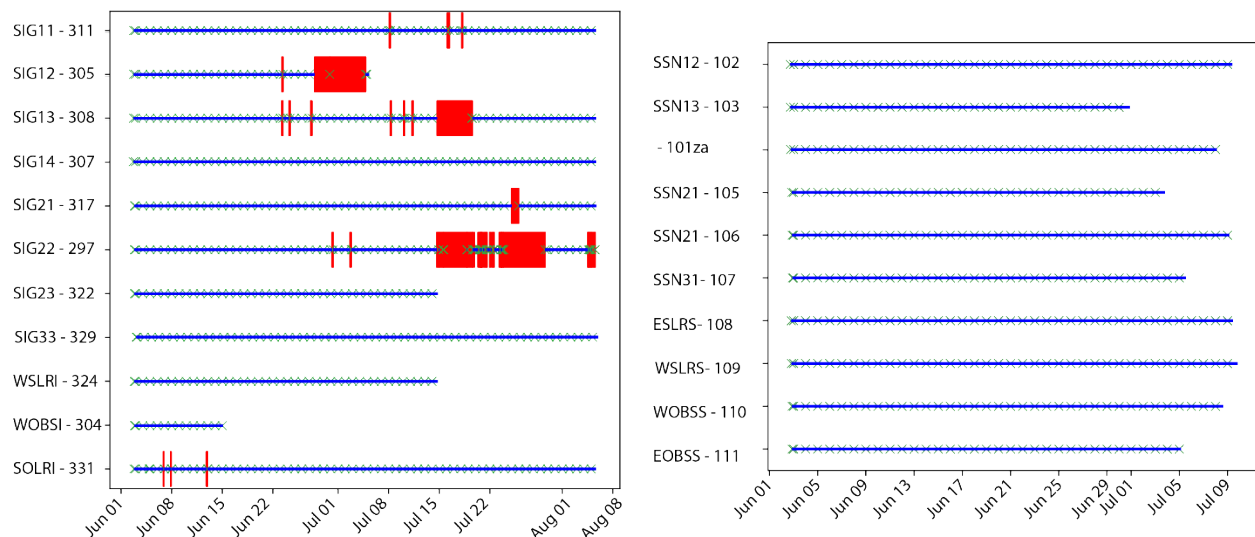


Figure 2: Data continuity for seismic (left) and infrasound (right) stations. Vertical redlines indicate gaps in the data; blue lines indicate continuous data. Green x's indicate a new day.

Table 1: Deployment details for the ThunderDOEME deployment.

Name	Instrument	Latitude	Longitude	Serial Number	Node Line	Start Date	End Date
ESLRI	GEM	33.9880529	-107.18233	156	-	-	-
SIG31	GEM	33.9758537	-107.18413	208	-	-	-
SIG32	GEM	33.9752001	-107.18479	209	-	-	-
EOBSI	GEM	33.9754674	-107.18172	210	-	-	-
SIG22	GEM	33.9824317	-107.18753	297	-	6/3/25	8/5/25
WOBSI	GEM	33.9789182	-107.19386	304	-	6/3/25	6/15/25
SIG12	GEM	33.9897199	-107.18788	305	-	6/3/25	7/5/25
SIG14	GEM	33.9891564	-107.18717	307	-	6/3/25	8/5/25
SIG13	GEM	33.9899486	-107.18686	308	-	6/3/25	8/5/25
SIG11	GEM	33.9905401	-107.18758	311	-	6/3/25	8/5/25
SIG21	GEM	33.9816716	-107.18811	317	-	6/3/25	8/5/25
SIG23	GEM	33.9826074	-107.18867	322	-	6/3/25	7/14/25
WSLRI	GEM	33.9877823	-107.19205	324	-	6/3/25	7/14/25
SIG33	GEM	33.975016	-107.18376	329	-	6/3/25	8/5/25
SOLRI	GEM	33.991555	-107.18831	331	-	6/3/25	8/5/25
SSN11	Node	33.9905272	-107.18759	0	104	-	-
SSN12	Node	33.9897127	-107.18789	3445	102	6/3/25	7/9/25
SSN13	Node	33.9899374	-107.18686	5496	103	6/3/25	6/30/25
SSN14	Node	33.9891471	-107.18716	5462	101	6/3/25	7/8/25
SSN21	Node	33.9816443	-107.18808	6490	105	6/3/25	7/3/25
SSN31	Node	33.9758673	-107.18412	5508	106	6/3/25	7/9/25
ESLRS	Node	33.9880837	-107.18235	679	107	6/3/25	7/5/25
SOLRS	Node	33.9915042	-107.1883	5448	108	6/3/25	7/9/25
WSLRS	Node	33.9877654	-107.19204	5493	109	6/3/25	7/9/25
WOBSS	Node	33.9789128	-107.19386	3447	110	6/3/25	7/8/25
EOBSS	Node	33.9754565	-107.18172	5485	111	6/3/25	7/5/25

3. DATA

Throughout the duration of the deployment three triggered lightning events were executed. The rocket launch method for triggering lightning involved using a rocket equipped with a copper wire. The wire acts as a conductive path, allowing the electric field around the wire to ionize the air and initiate a lightning strike. As a first pass at this dataset, we use these events, which have a known ground-truth time associated with them, to show examples of thunder on the seismic and infrasound recordings.

On June 11th, two lightning events were triggered at approximately 21:04 and 21:06 UTC. All the deployed instrumentation was operational during this time. Clear thunder arrivals can be seen in the waveforms for nearly all stations (Figure 3 & 4). For the infrasound this signal is likely the acoustic wave of the thunder, while for the seismic this signal likely represents the infrasound coupling with the ground, resulting in a ground-coupled airwave (Lin and Langston, 2007). For the first event, peak frequencies of the observed signals ranged from \sim 4 to 13 Hz for the infrasound signals and from 5 to 17 Hz for the seismic signals. The second event has higher peak frequencies across both phenomena, with the infrasound signals ranging from \sim 5 to 18 Hz and the seismic signals ranging from 6 to 40 Hz.

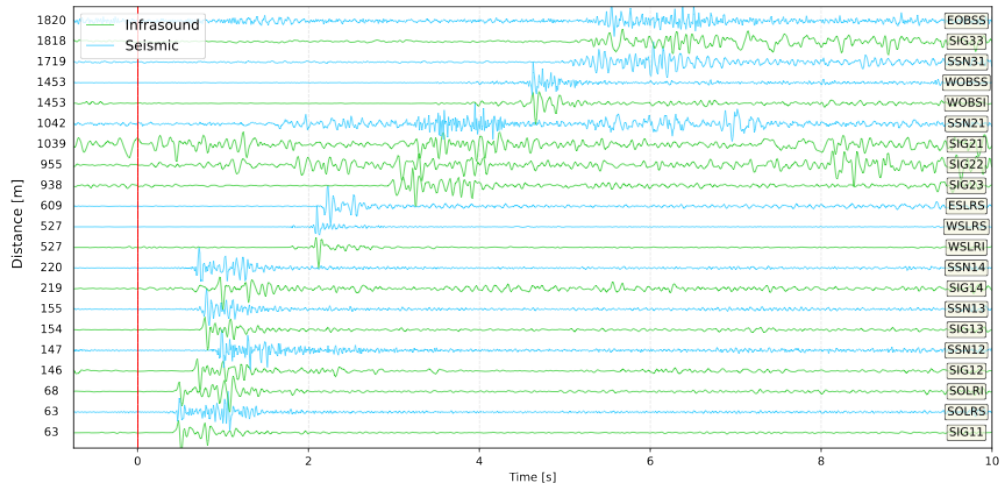


Figure 3: Record section showing infrasound and seismic waveforms following the June 10th 21:04 UTC triggered lightning strike. Blue traces are the vertical component seismogram, and green traces are the infrasound trace. Distances are calculated using the surface location of the rocket launch as the origin location and the origin time estimate (red line) based on electric field instrumentation. Traces are filtered using a 1–25 Hz bandpass. Distances are sorted sequentially by increasing distance, but relative distance is not incorporated to clearly show the individual waveforms.

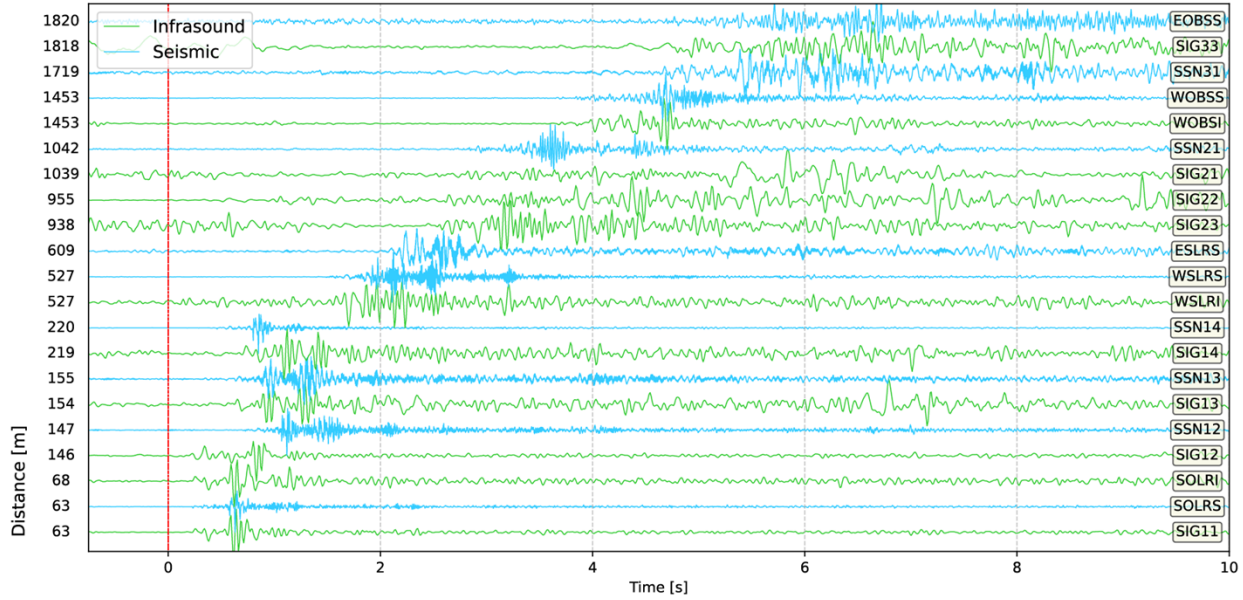


Figure 4: Record section showing infrasound and seismic waveforms following the June 10th 21:06 UTC triggered lightning strike. All other parameters are as in Figure 3.

A third triggered lightning strike occurred July 18th at 19:45. At this point only five of the GEMs and no seismometers were still recording. The frequencies for this event range from \sim 6 to 12 Hz. Figure 5 shows the data for the available stations.

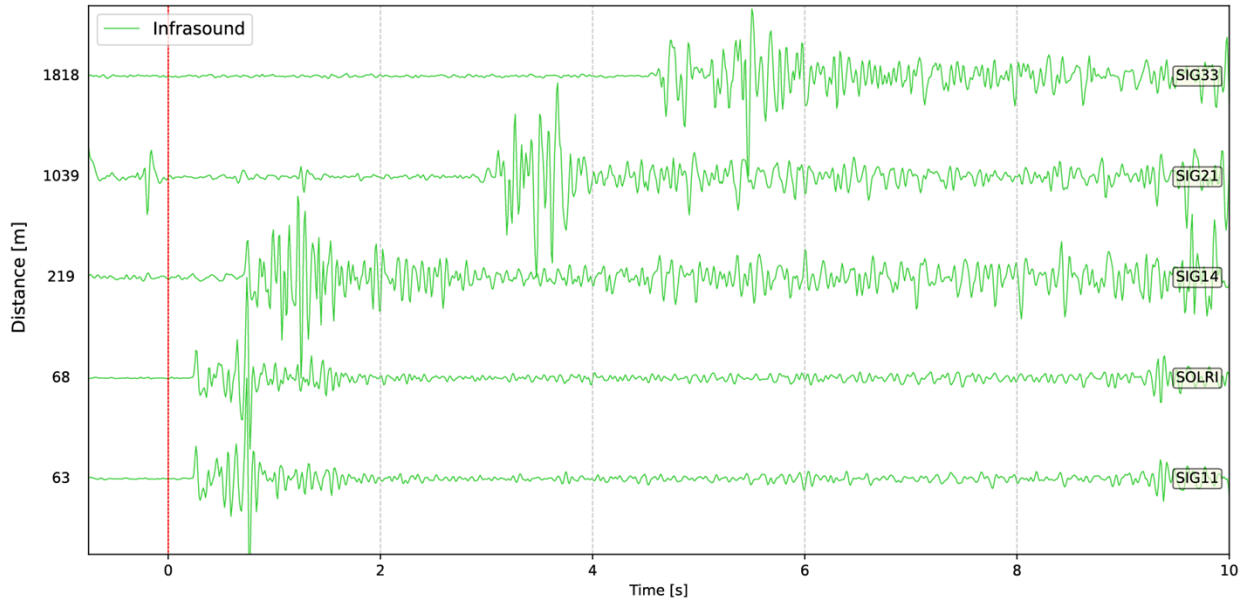


Figure 5: Record section showing infrasound waveforms following the July 18th 19:45 UTC triggered lightning strike. All other parameters are as in Figure 3.

In addition to the triggered strikes, optical and EM sensors also provided detections of 480 untriggered lightning strikes, providing an unprecedented opportunity to explore thunder in seismic and infrasound data. While we do not explore these detections further here, Figure 6 shows a

30-minute period with lightning detections from an optical sensor alongside the seismic and infrasound data. Clear thunder signals can be observed following many of the lightning detections. In addition, there are signals not following a lightning detection that may represent thunder signals not recorded by the electric field instruments. Previous work has suggested the electric field sensors can identify signals out to ~ 24 km, so these may represent thunder signals from greater distances (Leal, 2021), suggesting that missed detections indicate further sources. Across this 30-minute window there is a strong similarity between the seismic and acoustic traces. Additionally, across all three components, amplitudes seem consistent.

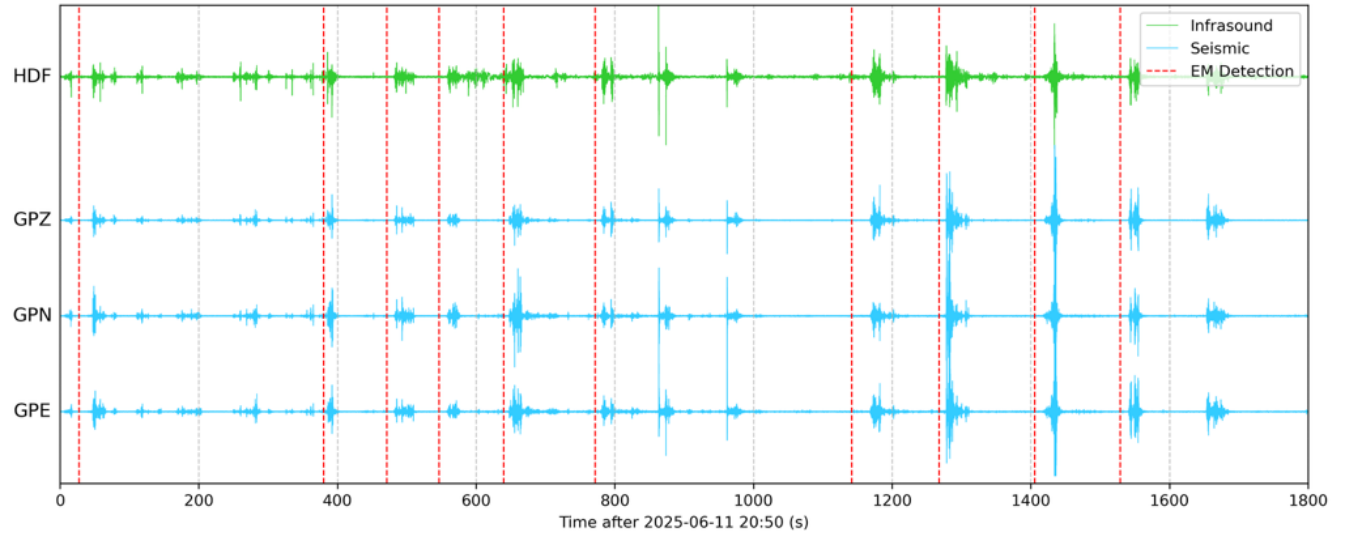


Figure 6: Infrasound and seismic waveforms for a 30-minute period during a thunderstorm on June 11th. Dashed red lines indicate lightning detections from electric field instrumentation, green trace is infrasound station SIG11, and blue is seismic station SSN14. Seismic traces are normalized across all components.

4. CONCLUSIONS

This report documents the successful deployment of seismic and acoustic instruments at the Langmuir Observatory in the Magdalena Mountains, southwest of Socorro, New Mexico, aimed at capturing thunder signals. The infrasound sensors recorded data for up to two months, while the seismic sensors maintained an average operational duration of approximately 34 days. A first look at the data indicates that clear thunder signals are prevalent in both the seismic and infrasound datasets, demonstrating the effectiveness of the deployed instrumentation in capturing these phenomena. Additionally, the human-triggered lightning strikes conducted throughout the deployment have enriched the dataset, allowing a more precise correlation between lightning events and the resulting acoustic signals. The dataset, which includes over 400 lightning detections, presents an unprecedented opportunity for further exploration of thunder signals and their characteristics. Future work could involve a more detailed analysis of the acoustic-to-seismic coupling mechanisms, as well as the potential for distinguishing between natural and anthropogenic noise sources.

REFERENCES

Anderson, J. F., Johnson, J. B., Bowman, D. C., & Ronan, T. J. (2018). The Gem infrasound logger and custom-built instrumentation. *Seismological Research Letters*, 89(1), 153-164.

Farges, T., Hupe, P., Le Pichon, A., Ceranna, L., Listowski, C., & Diawara, A. (2021). Infrasound Thunder Detections across 15 Years over Ivory Coast: Localization, Propagation, and Link with the Stratospheric Semi-Annual Oscillation. *Atmosphere*, 12(9), 1188. <https://doi.org/10.3390/atmos12091188>

Hong, T.-K., Park, S., Chung, D., & Kim, B. (2022). Inversion of acoustic thunder source spectral model from thunder-induced seismic waves in megacity. *Geophysical Journal International*, 233(1), 107–126. <https://doi.org/10.1093/gji/ggac440>

Lin, T., & Langston, C. A. (2007). Infrasound from thunder: A natural seismic source. *Geophysical Research Letters*, 34(14), 2007GL030404. <https://doi.org/10.1029/2007GL030404>

Lin, T., & Langston, C. A. (2009). Thunder-induced ground motions: 1. Observations. *Journal of Geophysical Research: Solid Earth*, 114(B4), 2008JB005769. <https://doi.org/10.1029/2008JB005769>

Lin, T. L., & Langston, C. A. (2009). Thunder-induced ground motions: 2. Site characterization. *Journal of Geophysical Research: Solid Earth*, 114(B4).

Leal, A. F. (2021, September). Remote measurements of lightning return stroke peak currents based on electric and acoustic signals. In 2021 35th International Conference on Lightning Protection (ICLP) and XVI International Symposium on Lightning Protection (SIPDA) (Vol. 1, pp. 1-6). IEEE.

Scamfer, L. T., & Anderson, J. F. (2023). Exploring Background Noise With a Large-N Infrasound Array: Waterfalls, Thunderstorms, and Earthquakes. *Geophysical Research Letters*, 50(24), e2023GL104635. <https://doi.org/10.1029/2023GL104635>

This page left blank

DISTRIBUTION

Email—Internal

Name	Org.	Sandia Email Address
Clinton Koch	6756	clikoch@sandia.gov
Bill O'Rourke	5447	wtorour@sandia.gov
Erika Vreeland	6633	ecooley@sandia.gov
Michael Fleigle	6752	mjfleig@sandia.gov
Nora Wynn	6752	nwynn@sandia.gov
Technical Library	1911	sanddocs@sandia.gov

Email—External

Name	Company Email Address	Company Name

Hardcopy—Internal

Number of Copies	Name	Org.	Mailstop

Hardcopy—External

Number of Copies	Name	Company Name and Company Mailing Address

This page left blank

This page left blank



**Sandia
National
Laboratories**

Sandia National Laboratories is a multimission laboratory managed and operated by National Technology & Engineering Solutions of Sandia LLC, a wholly owned subsidiary of Honeywell International Inc. for the U.S. Department of Energy's National Nuclear Security Administration under contract DE-NA0003525.